

# ACTIVE TUNING

**Sebastian Otte, Matthias Karlbauer, & Martin V. Butz**

Neuro-Cognitive Modeling  
University of Tübingen  
Sand 14, 72076 Tübingen, Germany

## ABSTRACT

We introduce Active Tuning, a novel paradigm for optimizing the internal dynamics of recurrent neural networks (RNNs) on the fly. In contrast to the conventional sequence-to-sequence mapping scheme, Active Tuning decouples the RNN’s recurrent neural activities from the input stream, using the unfolding temporal gradient signal to tune the internal dynamics into the data stream. As a consequence, the model output depends only on its internal hidden dynamics and the closed-loop feedback of its own predictions; its hidden state is continuously adapted by means of the temporal gradient resulting from backpropagating the discrepancy between the signal observations and the model outputs through time. In this way, Active Tuning infers the signal actively but indirectly based on the originally learned temporal patterns, fitting the most plausible hidden state sequence into the observations. We demonstrate the effectiveness of Active Tuning on several time series denoising benchmarks, including multiple super-imposed sine waves, a chaotic double pendulum, and spatiotemporal wave dynamics. Active Tuning consistently improves the robustness, accuracy, and generalization abilities of all evaluated models. Moreover, networks trained for signal prediction and denoising can be successfully applied to a much larger range of noise conditions with the help of Active Tuning. Thus, given a capable time series predictor, Active Tuning enhances its online signal filtering, denoising, and reconstruction abilities without the need for additional training.

## 1 INTRODUCTION

Today’s recurrent neural networks (RNNs) are not very robust against noise and often generate unsuitable predictions when confronted with corrupted or missing data (cf., e.g., Otte et al., 2015). To tackle noise, an explicit noise-aware training procedure can be employed, yielding denoising networks, which are targeted to handle particular noise types and levels. Recurrent oscillators, such as echo state networks (ESNs) (Jaeger, 2001; Koryakin et al., 2012; Otte et al., 2016), when initialized with teacher forcing, however, are highly dependent on a clean and accurate target signal. Given an overly noisy signal, the system is often not able to tune its neural activities into the desired target dynamics at all. Here, we present a method that can be seen as an alternative to regular teacher forcing and, moreover, as a general tool for more robustly tuning and thus synchronizing the dynamics of a generative differentiable temporal forward model—such as a standard RNN, ESN, or LSTM-like RNN (Hochreiter & Schmidhuber, 1997; Otte et al., 2014; Chung et al., 2014; Otte et al., 2016)—into the observed data stream.

The proposed method, which we call Active Tuning, uses gradient back-propagation through time (BPTT) (Werbos, 1990), where the back-propagated gradient signal is used to tune the hidden activities of a neural network instead of adapting its weights. The way we utilize the temporal gradient signal is related to learning parametric biases (Sugita et al., 2011) and applying dynamic context inference (Butz et al., 2019).

With Active Tuning, two essential aspects apply: First, during signal inference, the model is not driven by the observations directly, but indirectly via prediction error-induced temporal gradient information, which is used to infer the hidden state activation sequence that best explains the observed signal. Second, the general stabilization ability of propagating signal hypotheses through the network is exploited, effectively washing out activity components (such as noise) that cannot be

modeled with the learned temporal structures within the network. As a result, the vulnerable internal dynamics are kept within a system-consistent activity milieu, effectively decoupling it from noise or other unknown distortions that are present in the defective actual signal. In this work we show that Active Tuning elicits enhanced signal filtering abilities, without the need for explicitly training distinct models for exactly such purposes. Excitingly, this method allows for instance the successful application of an entirely noise-unaware RNN (trained on clean, ideal data) under highly noisy and unknown conditions.

In the following, we first detail the Active Tuning algorithm. We then evaluate the RNN on three time series benchmarks—multiple superimposed sinewaves, a chaotic pendulum, and spatiotemporal wave dynamics. The results confirm that Active Tuning enhances noise robustness in all cases. The mechanism mostly even beats the performance of networks that were explicitly trained to handle a particular noise level. In conclusion, we recommend to employ Active Tuning in all time series prediction cases, when the data is known to be noisy, corrupted, or to contain missing values and the generative differentiable temporal forward model—typically a particular RNN architecture—knows about the potential underlying system dynamics. The resulting data processing system will be able to handle a larger range of noise and corrupted data, filtering the signal, generating more accurate predictions, and thus identifying the underlying data patterns more accurately and reliably.

## 2 ACTIVE TUNING

Starting point for the application of Active Tuning is a trained temporal forward model. This may be, as mentioned earlier, an RNN, but could also be another type of temporal model. The prerequisite is, however, a differentiable model that implements dependencies over time, such that BPTT can be used to reversely route gradient information through the computational forward chain. Without loss of generality, we assume that the model of interest, whose forward function may be referred to as  $f_M$ , fulfills the following structure:

$$(\boldsymbol{\sigma}^t, \mathbf{x}^t) \xrightarrow{f_M} (\boldsymbol{\sigma}^{t+1}, \tilde{\mathbf{x}}^{t+1}), \quad (1)$$

where  $\boldsymbol{\sigma}^t$  is the current latent hidden state of the model (e.g. the hidden outputs of LSTM units, their cell states, or any other latent variable of interest) and  $\mathbf{x}^t$  is the current signal observation. Based on this information  $f_M$  generates a prediction for the next input  $\tilde{\mathbf{x}}^{t+1}$  and updates its latent state  $\boldsymbol{\sigma}^{t+1}$  accordingly.

Following the conventional inference scheme, we feed a given sequence time step by time step into the network and receive a one-time step ahead prediction after each particular step. Over time, this effectively synchronizes the network with the observed signal. Once the network dynamics are initialized, which is typically realized by teacher forcing, the network can generate prediction and its dynamics can be driven further into the future in a closed-loop manner, whereby the network feeds itself with its own predictions. To realize next time step- and closed-loop predictions, direct contact with the signal is inevitable to drive the teacher forcing process. In contrast, Active Tuning decouples the network from the direct influence of the signal. Instead, the model is permanently kept in closed-loop mode, which initially prevents the network from generating meaningful predictions. Over a certain time frame, Active Tuning keeps track of the recent signal history, the recent hidden states of the model, as well as its recent predictions. We call this time frame (retrospective) tuning horizon or tuning length (denoted with  $R$ ).

The principle of Active Tuning can best be explained with the help of Figure 1. With every new perceived and potentially noise-affected signal observation  $\mathbf{x}^t$ , one or multiple tuning cycles are performed. Every tuning cycle hereby consists of the following stages: First, from the currently believed sequence of signal predictions (which is in turn based on a sequence of hidden states) and the actual observed recent inputs, a prediction error is calculated and propagated back into the past reversely along the unfolded forward computation sequence. The temporal gradient travels to the very left of the tuning horizon and is finally projected onto the seed hidden state  $\boldsymbol{\sigma}^{t-R}$ , which is then adapted by applying the gradient signal in order to minimize the encountered prediction error. This adaption can be done using any gradient-based optimizer. Note that in this paper, we exclusively use Adam (Kingma & Ba, 2015), but other optimizers are possible as well. Second, after the adaption of this seed state (and maybe the seed input as well) the prediction sequence is rolled out from the

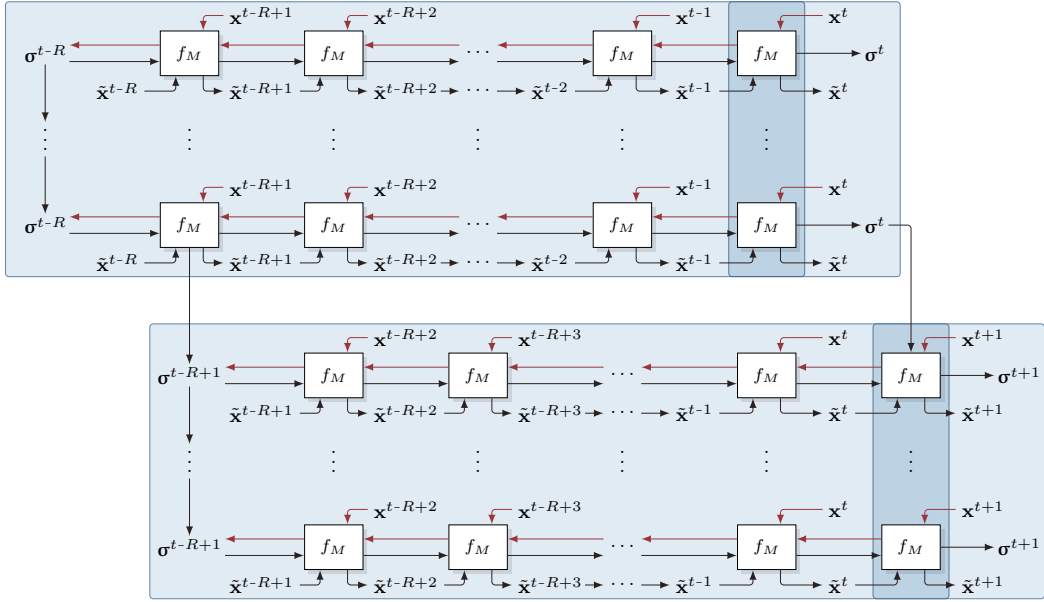


Figure 1: Illustration of the procedure behind Active Tuning for two consecutive world time steps.  $f_M$  refers to the forward pass of the model of interest.  $x^t, x^{t-1}$  etc. are the recent potentially noise-affected signal observations, whereas  $\tilde{x}^t, \tilde{x}^{t-1}$  etc. are the respective predictions (outputs of the model’s forward function  $f_M$ ).  $R$  denotes the length of the retrospective tuning horizon, that is, the number of time steps the prediction error is projected back into the past using BPTT.  $\sigma^{t-R}$  refers to the latent (hidden) state of  $M$  at the beginning of the tuning horizon, which essentially seeds the unfolding prediction sequence (black lines).  $\sigma^{t-R}$  is actively optimized based on the back-projected prediction error gradient (red lines).

past into the present again, effectively refining the output sequence towards a better explanation of the recently observed signal.

Each tuning cycle thus updates the current prediction  $\tilde{x}^t$  and the current hidden state  $\sigma^t$  from which a closed-loop future prediction can be rolled out, if desired. To transition into the next world time step, one forward step has to be computed. The formerly leftmost seed states can be discarded and the recorded history is shifted by one time step, making  $\sigma^{t-R+1}$  the new seed state that will be tuned within the next world time step.

From then on, the procedure is repeated, yielding the continuous adaptive tuning process. As a result, the model is predominantly driven by its own imagination, that is, its own top down predictions. Meanwhile, the predictions themselves are adapted by means of the temporal gradients based on the accumulated prediction error, but not by the signal directly. In a nutshell, Active Tuning realizes a gradient-based mini-optimization procedure on any of the model’s latent variables within one world time step. While it needs to be acknowledged that this process draws on additional computational resources, in this paper we investigate the resulting gain in signal processing robustness in the case of noisy data.

Intuitively speaking, Active Tuning tries to fit known temporal patterns, as memorized within the forward model, to the concurrently observed data. Due to the strong pressure towards consistency maintenance, which is naturally enforced by means of the temporal gradient information in combination with the repeatedly performed forward passes of the hidden state activities, the network will generate adaptations and potential recombinations of patterns that it has learned during training. Occurrences that cannot be generated from the repertoire of neural dynamics will therefore not appear (or only in significantly suppressed form) in the model’s output. As a consequence, there is a much smaller need to strive for noise robustness during training. Our results below indeed confirm that the model may be trained on clean, idealized target signals. However, imprinting a slight denoising tendency during training proves to be useful when facing more noisy data. Enhanced with our Active Tuning scheme, the model will be able to robustly produce high-quality outputs even

under extremely adverse conditions—as long as (some of) the assumed target signals are actually present. Our scheme is thus a tool that can be highly useful in various application scenarios for signal reconstruction and flexible denoising.

### 3 EXPERIMENTS

In order to investigate the abilities of Active Tuning we studied its behavior at considering three different types of time series data, namely, one-dimensional linear dynamics, two-dimensional non-linear dynamics, and distributed spatiotemporal dynamics. For all three problem domains we used a comparable setup except for the particular recurrent neural network architectures applied. We trained the networks as one time step ahead predictors whose task is to predict the next input given both the current input and the history of inputs aggregated in the latent hidden state of the models. The target sequences were generated directly from the clean input sequences by realizing a shift of one time step. Moreover, we trained networks under six different denoising conditions (normally distributed) per experiment, where we fed a potentially noisy signal into the network and provide the true signal (one time step ahead) as the target value (Lu et al., 2013; Otte et al., 2015; Goodfellow et al., 2016). These conditions are determined by their relative noise ratios: 0.0 (no noise), 0.05, 0.1, 0.2, 0.5, and 1.0, where the ratios depend on the respective base signal statistics. For instance, a noise ratio of 0.1 means that the noise added to the input has a standard deviation of 0.1 times the standard deviation of the base signal. As a result we obtained predictive *denoising experts* for each of these conditions. All models were trained with Adam (Kingma & Ba, 2015) using its default parameters (learning rate  $\eta = 0.001$ ,  $\beta_1 = 0.9$  and  $\beta_2 = 0.999$ ) over 100 (first two experiments) or 200 (third experiment) epochs, respectively.

#### 3.1 MULTI-SUPERIMPOSED OSCILLATOR

The first experiment is a variant of the *multiple superimposed oscillator* (MSO) benchmark (Schmidhuber et al., 2007; Koryakin et al., 2012; Otte et al., 2016). Multiple sine waves with different frequencies, phase-shifts, and amplitudes are superimposed into one signal:

$$\text{MSO}_n(t) = \sum_{i=1}^n a_i \sin(f_i t + \varphi_i) \quad (2)$$

where  $n$  gives the number of superimposed waves,  $f_i$  the frequency,  $a_i$  the amplitude, and  $\varphi_i$  the phase-shift of each particular wave, respectively. Typically, the task on this benchmark is to predict the further progression of the signal given some initial data points (e.g. the first 100 time steps) of the sequence. The resulting dynamics are comparably simple as they can, in principle, be learned with a linear model. It is, however, surprisingly difficult for BPTT-based models, namely LSTM-like RNNs, to precisely continue a given sequence for more than a few time steps (Otte et al., 2019).

For this experiment we considered the  $\text{MSO}_5$  dynamics with the default frequencies  $f_1 = 0.2$ ,  $f_2 = 0.311$ ,  $f_3 = 0.42$ ,  $f_4 = 0.51$ , and  $f_5 = 0.63$  (see the ground truth in Figure 3 for an example). For training, we generated 10 000 examples with 400 time steps each, using random amplitudes  $a_i \sim [0, 1]$  and random phase-shifts  $\varphi_i \sim [0, 2\pi]$ . For testing, another 1 000 examples were generated. As base model, we used an LSTM network with one input, 32 hidden units, one linear output neuron, and no biases.

#### 3.2 CHAOTIC PENDULUM

The second experiment is based on the simulation of a chaotic double pendulum. As illustrated in Figure 2, the double pendulum consists of two joints whose angles are specified by  $\theta_1$  and  $\theta_2$  and two rods of length  $l_1$  and  $l_2$ . Besides the length of the rods, the masses  $m_1$  and  $m_2$  affect the behavior of the pendulum. The pendulum’s end-effector (where  $m_2$  is attached) generates smooth, but highly non-linear trajectories. More precisely, it exhibits chaotic behavior, meaning that already slight changes of the current system state can quickly cause major changes of the pendulum’s state (Korsch et al., 2008; Pathak et al., 2018). It is thus typically difficult to precisely predict the dynamics of such a system for more than a few time steps into the future, making it a challenging benchmark problem for our purposes.

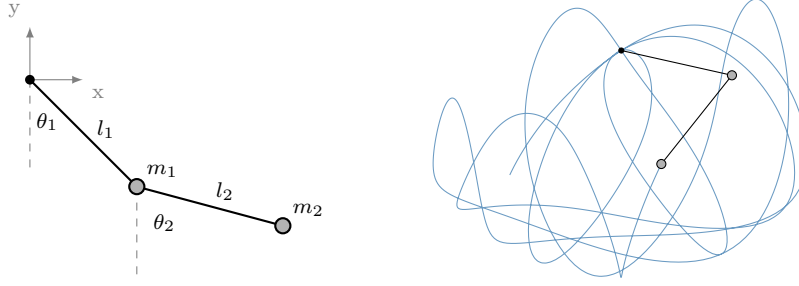


Figure 2: The double pendulum used for data generation of the second experiment and a resulting nonlinear trajectory of the pendulum's end-effector.

In the literature, the double pendulum's dynamics are typically described using the equations of motion, given by Equation 3 and Equation 4, respectively, which are derived from the Lagrangian of the system and the Euler-Lagrange equations; see Korsch et al. (2008) for details.

$$\ddot{\theta}_1 = \frac{\mu g_1 \sin(\theta_2) \cos(\theta_2 - \theta_1) + \mu \dot{\theta}_1^2 \sin(\theta_2 - \theta_1) \cos(\theta_2 - \theta_1) - g_1 \sin(\theta_1) + \frac{\mu}{\lambda} \dot{\theta}_2^2 \sin(\theta_2 - \theta_1)}{1 - \mu \cos^2(\theta_2 - \theta_1)} \quad (3)$$

$$\ddot{\theta}_2 = \frac{g_2 \sin(\theta_1) \cos(\theta_2 - \theta_1) - \mu \dot{\theta}_2^2 \sin(\theta_2 - \theta_1) \cos(\theta_2 - \theta_1) - g_2 \sin(\theta_2) - \lambda \dot{\theta}_1^2 \sin(\theta_2 - \theta_1)}{1 - \mu \cos^2(\theta_2 - \theta_1)}, \quad (4)$$

where

$$\lambda = \frac{l_1}{l_2}, \quad g_1 = \frac{g}{l_1}, \quad g_2 = \frac{g}{l_2}, \quad \mu = \frac{m_2}{m_1 + m_2},$$

and  $g = 9.81$  being the gravitational constant. For simulating the double pendulum, we applied the fourth-order Runge-Kutta (RK4) (Press, 2007) method to numerically integrate the equations of motion. All four parameters  $l_1$ ,  $l_2$ ,  $m_1$ , and  $m_2$  were set to 1.0. A temporal step size of  $h = 0.01$  was chosen for numerical integration. The initial state of the pendulum is described by its two angles, which were selected randomly for each sample to be within  $\theta_1 \sim [90^\circ, 270^\circ]$  and  $\theta_2 \sim [\theta_1 \pm 30^\circ]$  to ensure sufficient energy in the system. One out of ten sequences was initiated with zero angle momenta, that is  $\dot{\theta}_1, \dot{\theta}_2 = 0.0$ . The number of train and test samples, as well as the sequence lengths were chosen analogously to experiment one. As base model we used an LSTM network with two inputs, 32 hidden units, two linear output neurons, and again no biases.

### 3.3 SPATIOTEMPORAL WAVE DYNAMICS

In the third experiment we considered a more complex spatiotemporal wave propagation process, based on the following wave equation:

$$\frac{\partial^2 u}{\partial t^2} = c^2 \left( \frac{\partial^2 u}{\partial x^2} + \frac{\partial^2 u}{\partial y^2} \right). \quad (5)$$

This equation was solved numerically using the method of second order central difference, yielding

$$u(x, y, t + h_t) \approx c^2 h_t^2 \left( \frac{\partial^2 u}{\partial x^2} + \frac{\partial^2 u}{\partial y^2} \right) + 2u(x, y, t) - u(x, y, t - h_t) \quad (6)$$

with, after solving  $\partial^2 u / \partial x^2$  and analogously  $\partial^2 u / \partial y^2$  via the same method,

$$\frac{\partial^2 u}{\partial x^2} = \frac{u(x + h_x, y, t) - 2u(x, y, t) + u(x - h_x, y, t)}{h_x^2}, \quad (7)$$

$$\frac{\partial^2 u}{\partial y^2} = \frac{u(x, y + h_y, t) - 2u(x, y, t) + u(x, y - h_y, t)}{h_y^2}. \quad (8)$$

Here,  $x$  and  $y$  correspond to the spatial position in the simulated field, while  $t$  denotes the time step and  $c = 3.0$  the propagation speed factor of the waves. The temporal and spatial approximation step

Table 1: MSO results (RMSE)

Inference (signal noise)	Training (signal noise)						
	Regular inference					Active Tuning	
	0.0	0.1	0.2	0.5	1.0	0.0	0.05
0.0	<b>0.0039</b>	0.0498	0.0781	0.1526	0.2383	—	—
0.1	0.5880	0.0966	0.0993	0.1579	0.2397	<b>0.0912</b>	0.0947
0.2	1.0336	0.1734	<b>0.1454</b>	0.1728	0.2446	0.1682	0.1550
0.5	1.8713	0.4265	0.3190	<b>0.2538</b>	0.2751	0.3583	0.3611
1.0	2.6241	0.9502	0.6437	0.4396	<b>0.3639</b>	0.5699	0.6101

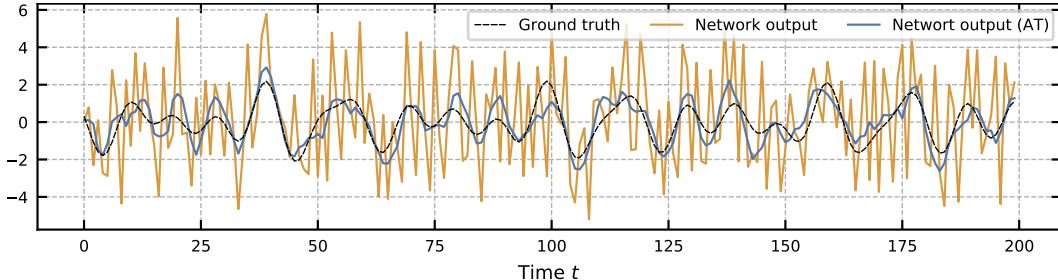


Figure 3: Visual comparison of regular inference (orange) vs. Active Tuning (light blue) on an MSO example with strong noise (noise ratio 1.0) using a noise-unaware LSTM.

sizes were set to  $h_t = 0.1$  and  $h_x = h_y = 1.0$ , respectively. No explicit boundary condition was applied, resulting in the waves being reflected at the borders and the overall energy staying constant over time. We generated sequences for a regular grid of  $16 \times 16$  pixels (see Figure 5 for illustrations of the two-dimensional wave). In contrast to the previous two experiments, 200 samples with a sequence length of 80 were generated for training, whereas 20 samples over 400 time steps were used for evaluation.

As base network we used a distributed graph-RNN called DISTANA (Karlbauer et al., 2020), which is essentially a mesh of the same RNN module (an LSTM, which consists here of four units only), which is distributed over the spatial dimensions of the problem space (here a two-dimensional grid), where neighboring modules are laterally connected. We chose this wave benchmark, and this recurrent graph network in particular, to demonstrate the effectiveness of Active Tuning in a setup of higher complexity.

## 4 RESULTS AND DISCUSSION

The quantitative evaluations are based on the root mean square error (RMSE) between the network outputs and the ground truth targets. The reported values are averages over ten independently randomized and trained models. In order to elaborate on the applicability of each denoising expert on unseen noise conditions, we evaluated all models using the noise ratios 0.0, 0.1, 0.2, 0.5, and 1.0, resulting in 25 baseline scores for each experiment. These baselines were compared on all noise ratios against eight Active Tuning setups, which were based on models trained without any noise (0.0) or with only a small portion of input noise (0.05), respectively. The individual parameters of Active Tuning that were used to produce the results are reported in Table 4, Table 5, and Table 6 of the appendix. Note that in all experiments, the latent hidden outputs of the LSTM units (not the cell states) were chosen as optimization target for the Active Tuning algorithm. Furthermore, these hidden states were initialized normally distributed with standard deviation 0.1 in all cases.

The results of the MSO experiment are summarized in Table 1. It appears that Active Tuning improves the results for the weakest model (0.0) in all cases (column 2 vs. column 7), partially almost by an order of magnitude. Noteworthy, for the inference noise ratio 0.1 the noise-unaware model becomes even better than the actual expert when driven with Active Tuning. Recall that there was no retraining of the model, only the paradigm how the models is applied to the data was changed. On the other hand, at least in this experiment, it seems that there is no advantage for Active Tuning when

Table 2: Pendulum results (RMSE)

Inference (signal noise)	Training (signal noise)						
	Regular inference					Active Tuning	
	0.0	0.1	0.2	0.5	1.0	0.0	0.05
0.0	<b>0.0091</b>	0.1475	0.2471	0.4459	0.5700	—	—
0.1	0.2097	0.1537	0.2489	0.4463	0.5702	0.0880	<b>0.0865</b>
0.2	0.4021	0.1711	0.2545	0.4474	0.5710	0.1423	<b>0.1284</b>
0.5	0.8458	0.2702	0.2945	0.4563	0.5764	0.2954	<b>0.2460</b>
1.0	1.2753	0.5308	0.4444	0.4918	0.5954	0.4868	<b>0.4030</b>

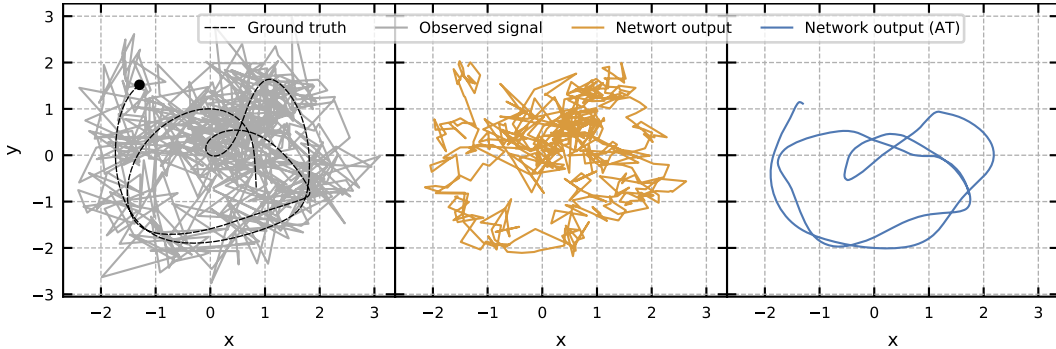


Figure 4: Exemplary comparison of regular inference (orange) vs. Active Tuning (light blue) on the double pendulum’s end-effector trajectory; the black dot denotes the start position. Here, the second strong noise condition (0.5) is shown, using a 0.05-noise LSTM for inference and Active Tuning.

the base network encountered minimal noise (0.05) during training. To get an impression of the actual improvement of the output quality, consider Figure 3. The noise-unaware model (0.0) produces very poor predictions when confronted with strong signal noise (1.0). Yet, when driven with Active Tuning instead of with regular inference (teacher forcing), the output of the same model is enhanced significantly, becomes smooth, and approximates the ground truth reasonably well. Active Tuning thus helps to catch most of the trend information while mostly ignoring noise.

For the pendulum experiment, the potential of Active Tuning becomes even more evident. The results presented in Table 2 indicate that for all noise ratios Active Tuning performs better than all experts, in particular, when applied to the model that was trained on small noise (0.05). Also noteworthy: with an increasing noise level, the problem apparently becomes impossible to learn, e.g. the 1.0-expert-model does not seem to provide any reasonable function at all, indicated by the worse RMSE score compared to other models (1.0 inference noise row). However, Active Tuning can handle these extremely unfavorable conditions surprisingly well. Figure 4 shows an exemplary case. The unknown ground truth is plotted against the noisy observations (shown in the left image). The center image shows the prediction of the reference LSTM (trained with 0.05 noise) when regular inference is applied. It is clearly difficult to recognize a coherent trajectory reflecting the dynamics of the double pendulum. In contrast, the same network driven with Active Tuning produced a mostly clean prediction that is relatively close to the ground truth sequence.

The results of the wave experiment reported in Table 3 consistently support the findings from the pendulum experiments. That is, (a) when driven with Active Tuning, all models were enhanced, producing even better results than the explicitly trained denoising experts on all noise levels, and (b) Active Tuning did unfold the largest potential when applied on a model that was trained on very small noise (0.05), reaching the best RMSE scores on all noise intensities. As shown in Figure 5 and in accordance with the previous experiments, the noisy signal observations (0.5) could be filtered effectively and latency-free (exclusively when using Active Tuning) to yield a smooth signal prediction across the entire spatiotemporal sequence. While the two-dimensional output of the network operating in conventional inference mode is hardly recognizable as a wave, the network output of the same model combined with Active Tuning clearly reveals the two-dimensional wave structure with hardly perceivable deviations from the ground truth.

Table 3: Wave results (RMSE)

Inference (signal noise)	Training (signal noise)						
	Regular inference					Active Tuning	
	0.0	0.1	0.2	0.5	1.0	0.0	0.05
0.0	<b>0.0007</b>	0.0021	0.0042	0.0096	0.0175	—	—
0.1	0.0268	0.0073	0.0064	0.0100	0.0176	0.0073	<b>0.0062</b>
0.2	0.0533	0.0142	0.0106	0.0113	0.0178	0.0097	<b>0.0087</b>
0.5	0.1295	0.0362	0.0262	0.0180	0.0197	0.0173	<b>0.0150</b>
1.0	0.2368	0.0784	0.2467	0.0345	0.0261	0.0283	<b>0.0213</b>

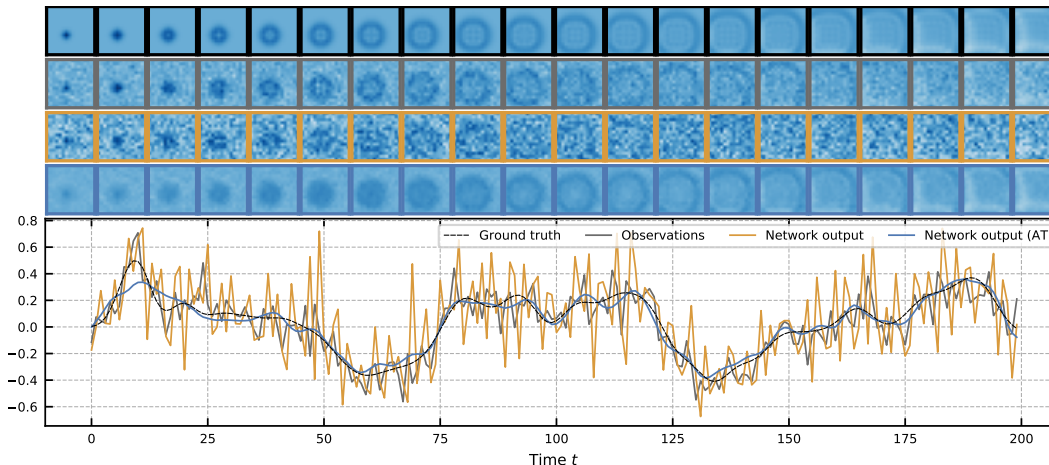


Figure 5: Exemplary comparison of regular inference (orange) vs. Active Tuning (light blue) on wave examples with strong noise (0.5) using DISTANA trained on weak noise (0.05). The four top rows visualize ground truth, noisy observations (network input), network output without, and network output with Active Tuning. The plot below shows the wave activities at the center position.

Note that we also performed experiments with other noise distributions (e.g. salt-and-pepper noise). Somewhat surprisingly the quality of the output was only marginally affected by this variation. Thus, in contrast to what is known about deep convolutional networks (Geirhos et al., 2018), the RNNs applied here apparently did not overfit to the noise type but only to the energy range of the noise.

## 5 CONCLUSION

In this work we augmented traditional RNN-based inference with Active Tuning, which decouples the internal dynamics of an RNN from the data stream. Instead of relying on the input signal to set the internal network states, Active Tuning uses the dynamic loss signal, which is projected onto the internal states, effectively tuning them. As a result, we have shown that RNNs driven with Active Tuning can reliably denoise various types of time series dynamics, mostly yielding higher accuracies than specifically trained denoising expert RNNs. In all cases, the augmentation with Active Tuning has beaten the standard RNN with teacher forcing.

Nonetheless, Active Tuning can in principle be mixed with traditional teacher forcing. We will investigate potential synergies in the future, especially switching teacher forcing on and off in an adaptive manner depending on the current signal conditions.

While we used a tuning length of up to 16 time steps with partially up to 30 tuning cycles, additional future research will aim at reducing these requirements. Ideally, Active Tuning will work reliably with a single update cycle over a tuning length of a single time step, which would allow to perform Active Tuning along with the regular forward pass of the model in a fused computation step. Additionally, we aim at applying Active Tuning to real-world denoising and forecasting challenges, including speech recognition and weather forecasting.

## REFERENCES

- Martin V. Butz, David Bilkey, Dania Humaidan, Alistair Knott, and Sebastian Otte. Learning, planning, and control in a monolithic neural event inference architecture. *Neural Networks*, 117: 135–144, 2019. doi: 10.1016/j.neunet.2019.05.001.
- Junyoung Chung, Caglar Gulcehre, KyungHyun Cho, and Yoshua Bengio. Empirical Evaluation of Gated Recurrent Neural Networks on Sequence Modeling. *arXiv:1412.3555 [cs]*, December 2014. arXiv: 1412.3555.
- Robert Geirhos, Carlos R. M. Temme, Jonas Rauber, Heiko H. Schütt, Matthias Bethge, and Felix A. Wichmann. Generalisation in humans and deep neural networks. In S. Bengio, H. Wallach, H. Larochelle, K. Grauman, N. Cesa-Bianchi, and R. Garnett (eds.), *Advances in Neural Information Processing Systems 31*, pp. 7538–7550. Curran Associates, Inc., 2018.
- Ian Goodfellow, Yoshua Bengio, and Aaron Courville. *Deep Learning*. MIT Press, Cambridge, MA, 2016.
- S. Hochreiter and J. Schmidhuber. Long Short-Term memory. *Neural Computation*, 9(8):1735–1780, November 1997. doi: 10.1162/neco.1997.9.8.1735.
- H. Jaeger. The ”echo state” approach to analysing and training recurrent neural networks. Technical Report GMD Report, 148, Fraunhofer Institute for Analysis and Information Systems AIS, Sankt Augustin, Germany, 2001.
- Matthias Karlbauer, Sebastian Otte, Hendrik P. A. Lensch, Thomas Scholten, Volker Wulfmeyer, and Martin V. Butz. Inferring, predicting, and denoising causal wave dynamics, 2020.
- Diederik P. Kingma and Jimmy L. Ba. Adam: A method for stochastic optimization. *3rd International Conference for Learning Representations*, abs/1412.6980, 2015.
- H. J. Korsch, H.-J. Jodl, and T. Hartmann. *Chaos: a program collection for the PC*. Springer, Berlin ; New York, 3rd rev. and enlarged ed edition, 2008. ISBN 978-3-540-74866-3.
- D. Koryakin, J. Lohmann, and M. V. Butz. Balanced echo state networks. *Neural Networks*, 36: 35–45, 2012. doi: 10.1016/j.neunet.2012.08.008.
- Xugang Lu, Yu Tsao, Shigeki Matsuda, and Chiori Hori. Speech enhancement based on deep denoising autoencoder. In *Interspeech*, volume 2013, pp. 436–440, 2013.
- S. Otte, M. Liwicki, and A. Zell. Dynamic Cortex Memory: Enhancing Recurrent Neural Networks for Gradient-Based Sequence Learning. In *Artificial Neural Networks and Machine Learning – ICANN 2014*, number 8681 in Lecture Notes in Computer Science, pp. 1–8. Springer International Publishing, September 2014. ISBN 978-3-319-11178-0, 978-3-319-11179-7.
- Sebastian Otte, Marcus Liwicki, and Andreas Zell. An Analysis of Dynamic Cortex Memory Networks. In *International Joint Conference on Neural Networks (IJCNN)*, pp. 3338–3345, Killarney, Ireland, July 2015. ISBN 978-1-4799-1959-8.
- Sebastian Otte, Martin V. Butz, Danil Koryakin, Fabian Becker, Marcus Liwicki, and Andreas Zell. Optimizing recurrent reservoirs with neuro-evolution. *Neurocomputing*, 192:128–138, June 2016. ISSN 0925-2312. doi: 10.1016/j.neucom.2016.01.088.
- Sebastian Otte, Patricia Rubisch, and Martin V. Butz. Gradient-based learning of compositional dynamics with modular rnns. In *Artificial Neural Networks and Machine Learning – ICANN 2019*, number 11727 in Lecture Notes in Computer Science, pp. 484–496. Springer International Publishing, September 2019. ISBN 978-3-030-30487-4.
- Jaideep Pathak, Alexander Wikner, Rebeckah Fussell, Sarthak Chandra, Brian R Hunt, Michelle Girvan, and Edward Ott. Hybrid forecasting of chaotic processes: Using machine learning in conjunction with a knowledge-based model. *Chaos: An Interdisciplinary Journal of Nonlinear Science*, 28(4):041101, 2018.

William Press. *Numerical recipes : the art of scientific computing*. Cambridge University Press, Cambridge UK ;;New York, 3rd ed. edition, 2007. ISBN 978-0-521-88068-8.

Juergen Schmidhuber, Daan Wierstra, Matteo Gagliolo, and Faustino Gomez. Training recurrent neural networks by evoluno. *Neural Computation*, 19:757–779, 2007.

Yuuya Sugita, Jun Tani, and Martin V Butz. Simultaneously emerging braitenberg codes and compositionality. *Adaptive Behavior*, 19:295–316, 2011. doi: 10.1177/1059712311416871.

P.J. Werbos. Backpropagation through time: what it does and how to do it. *Proceedings of the IEEE*, 78(10):1550–1560, 1990. ISSN 0018-9219. doi: 10.1109/5.58337.

## A APPENDIX

The two Active Tuning parameters (tuning length  $R$  and number of tuning cycles  $C$ ), as well as the parameters for state adaptation with the Adam optimizer (tuning rate  $\eta$ ,  $\beta_1$  and  $\beta_2$ ) for the application of Active Tuning on the different benchmarks and various noise combinations are reported in distinct tables below.

Table 4: Active Tuning parameters – MSO experiment

Training noise	Signal noise	Tuning length ( $R$ )	Tuning cycles ( $C$ )	$\eta$	$\beta_1$	$\beta_2$
0.0	0.1	8	10	0.005	0.9	0.99
0.0	0.2	8	10	0.005	0.9	0.99
0.0	0.5	14	10	0.006	0.9	0.99
0.0	1.0	16	10	0.004	0.5	0.99
0.05	0.1	8	10	0.008	0.9	0.99
0.05	0.2	8	12	0.005	0.5	0.999
0.05	0.5	14	10	0.007	0.9	0.99
0.05	1.0	16	10	0.006	0.5	0.9

Table 5: Active Tuning parameters – pendulum experiment

Training noise	Signal noise	Tuning length ( $R$ )	Tuning cycles ( $C$ )	$\eta$	$\beta_1$	$\beta_2$
0.0	0.1	8	10	0.005	0.9	0.99
0.0	0.2	8	10	0.005	0.9	0.99
0.0	0.5	8	10	0.004	0.5	0.99
0.0	1.0	12	10	0.004	0.5	0.9
0.05	0.1	8	10	0.008	0.9	0.99
0.05	0.2	8	10	0.005	0.5	0.99
0.05	0.5	8	10	0.004	0.5	0.99
0.05	1.0	12	10	0.005	0.5	0.9

Table 6: Active Tuning parameters – wave experiment

Training noise	Signal noise	Tuning length ( $R$ )	Tuning cycles ( $C$ )	$\eta$	$\beta_1$	$\beta_2$
0.0	0.1	7	10	0.01	0.9	0.999
0.0	0.2	5	17	$6 \times 10^{-5}$	0.0	0.999
0.0	0.5	4	20	$8 \times 10^{-5}$	0.0	0.999
0.0	1.0	7	30	$4 \times 10^{-5}$	0.0	0.999
0.05	0.1	8	12	0.012	0.9	0.999
0.05	0.2	5	17	$1 \times 10^{-4}$	0.0	0.999
0.05	0.5	4	20	$1 \times 10^{-4}$	0.0	0.999
0.05	1.0	7	30	$5 \times 10^{-5}$	0.0	0.999